Preprint of the paper which appeared in ZAMM · Z. angew. Math. Mech. **83** (2003) No. 10, 1–16

HARDT, M.; VON STRYK, O.

Dynamic modeling in the simulation, optimization, and control of bipedal and quadrupedal robots

Fundamental principles and recent methods for investigating the nonlinear dynamics of legged robot motions with respect to control, stability and design are discussed. One of them is the still challenging problem of producing dynamically stable gaits. The generation of fast walking or running motions requires methods and algorithms adept at handling the nonlinear dynamical effects and stability issues which arise. Reduced, recursive multibody algorithms, a numerical optimal control method, and new stability and energy performance indices are presented which are well-suited for this purpose. Difficulties and open problems are discussed along with numerical investigations into the proposed gait generation scheme. Our analysis considers both biped and quadrupedal gaits.

Keywords: legged locomotion, path planning, dynamic stability, robot dynamics, optimization, nonlinear programming, walking

1 Introduction

1.1 Nonlinear Dynamics of Legged Robot Motion

A precise modeling of legged locomotion systems requires high dimensional nonlinear dynamics, and it is thus a complex task to generate and control stable motions for such systems. Biped and quadruped constructions generally consist of a minimum of five bodies with two to six degrees of freedom per leg in addition to the six degrees of freedom corresponding to the base body in order to give the necessary amount of motion dexterity necessary for a wide range of movement. Dynamic model simplifications in previous work, however, have generally ranged from pendulum models [33] to multi-link planar models [7, 8, 19, 21] for bipeds and for quadrupeds [22] or to multi-link spatial models [28, 40]. Though these simplifications allow one to analyze certain predominant behaviors of the dynamic system, several other important features are lost. A complete and complex dynamical system description will contain much more of the significant dynamical effects; yet a control solution for these models based on an analytical approach is usually not possible and results must be sought for numerically.

The dynamic effects characterizing bipedal and quadrupedal motion may be further complicated by external disturbance factors and forces, quickly changing system goals, low friction conditions, a limited power source, and inexact sensor information resulting from fast movements and a changing environment. The work described in this paper is directed towards the generation of dynamic motions with these difficulties and performance objectives in mind. Fast motions are more susceptible to *instabilities*, in particular due to the hybrid switching nature of the dynamics whenever the leg contact conditions change. Many severe system *constraints* related to 'exterior' environmental conditions or 'interior' actuator limitations must additionally be considered. Legged systems often have changing *performance* criteria (functions of dynamic state and control quantities measuring the desired system behavior which ideally are minimized) depending upon whether efficiency, speed, or robustness is prioritized. One of this paper's goals is to argue that only a numerical modeling and optimization approach can presently tackle these difficult hurdles, and that the approach described here is particularly well-suited due to its computational efficiency and its proven capability to treat high-dimensional, complex dynamical systems.

1.2 Solutions for Multibody Dynamics of Legged Robot Models

Multibody dynamical models (MBS) for real legged systems are typically characterized by a high number of degrees of freedom, relatively few contact constraints or collision events, and a variety of potential ground contact models, actuator models, and mass-inertial parameter settings due to changing load conditions. Multibody dynamical models serve for the optimization of gait trajectories or in the tuning of construction design parameters as will be presented in Sects. 4.2 and 6. They also play an important role in simulation and feedback control (Sect. 5).

Closed-form dynamical expressions, i.e. as a set of ordinary differential equations (ODEs), are the most efficient form of evaluating the dynamics. They are not, however, well-suited to legged systems due to the many

changing kinematic and kinetic parameters and external force models which would require the frequent and time-consuming generation of new dynamic equations. Better suited is an approach which is similarly efficient (important due to the many degrees of freedom in such systems), but permits the easy interchangeability of parameters and the introduction of external forces without repeated extensive preprocessing. The use of recursive, numerical algorithms which satisfy these criteria are presented in Sect. 2.3. They are superior in efficiency to other non-recursive multibody approaches such as the composite rigid-body method and can be programmed in a highly modular manner as all calculations and parameters can occur as an exchange of information between links. Reduced dynamical approaches appropriate for legged robots are additionally presented in Sect. 2.4.

1.3 Dynamical Stability of Legged Robot Motion

It is indisputable that the problem of maintaining stability in legged systems undergoing fast locomotion has been the main obstacle in the construction of such systems. There has been a wide spectrum of different approaches in previous work for generating dynamically stable motions in bipeds and quadrupeds. Analytical methods used for designing controllers for dynamically stable motion such as in [19, 27, 33] usually rely on simplified models and are not yet at a stage where the various influencing dynamical effects (constraints) previously mentioned can be considered. Other gait planning schemes using models with 3-dimensional motion rarely consider the full complexity of the stabilizing potential of the torso sway motion or that of arm swinging which can be advantageous for increasing robustness and reducing power consumption. It is not without reason that even the most advanced bipedal, autonomous robots as the Honda humanoids walk relatively slow compared to a human. The 1.6 m tall P3 which was presented in 1997 after eleven years of research walks at a maximum speed of 2 km/h, and the 1.2 m tall ASIMO presented in 2000 was the first of the Honda humanoids being able to walk along curves while achieving a maximum speed of 1.6 km/h.

Standard approaches for constructing stable legged 3-D motions for bipeds [28, 40] generally rely on heuristic schemes. These approaches work well for *statically stable* gaits when the projected ground center of gravity is constrained to lie within the support polygon, the convex hull about the leg contact points: a purely kinematic measure of stability. Extensions to dynamic stability using a dynamic stability criterion is usually based on the Zero-Moment-Point (ZMP) [53], yet this criterion is limited in its ability to classify stability [17]. For example, this measure is not appropriate when one of the biped's feet is rolling about its edge as the ZMP will then lie on the boundary of the support polygon and provide little information about the system's stability. It is apparent though that the rolling motion of the feet plays an important role in fast walking and running. The numerical investigations performed in [21] indicate that without this property the double contact phase of biped walking does not have an energetical advantage. In the case of quadrupeds with point contacts, a similar problem occurs. Nonetheless, 3-D bipeds and quadrupeds have been constructed which perform dynamically stable walking and running [26, 52, 56], though due to excessive power consumption they were either not autonomous or required a substantial battery supply for only a short operational period. We present in Sect. 3 alternative stability as well as energy-based performance measures to be used for bipedal and quadrupedal gait generation.

1.4 Numerical Optimization and Feedback Control of Bipedal and Quadrupedal Robot Motions

Algebraic control strategies for legged systems cannot yet handle the high dimension and many modeling constraints present in the locomotion problem. Heuristic control methods, on the other hand, tend to have poor performance with respect to power efficiency and stability making these approaches unattractive for implementation in a fast-moving legged system. The remaining proven approach is the use of sophisticated numerical optimization schemes which can incorporate the numerous modeling constraints to generate optimal trajectories. The resulting trajectories may later be tracked or used to approximate a feedback controller in the portion of state space of interest.

In our efforts to achieve dynamically stable and efficient gaits for various biped and quadruped legged system constructions, we explore in this work a numerical optimization approach which minimize performance or stability objectives in the gait generation problem. Numerical optimization tools have advanced sufficiently [16, 50] such that all the above-mentioned modeling and stability constraints can be incorporated into the problem formulation together with a relatively complete dynamical model so as to obtain truly realistic energy-efficient, stable and fast motions. The optimization approach is based on a discretization of the control problem in time using direct collocation and its subsequent formulation as a nonlinear programming problem then solved with a sparse sequential quadratic programming algorithm. This approach has already been successfully applied for gait planning in bipeds in two dimensions [21] and for quadrupeds in [22].

2 Dynamic Modeling of Legged Locomotion

2.1 Biped and Quadruped Dynamics

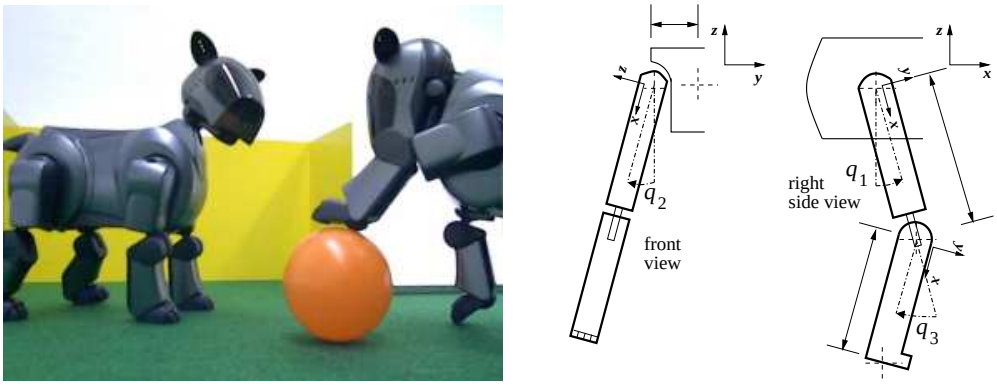

Figure 1: Four-legged Sony robots (left) used for RoboCup [10] and kinematical structure of one leg (right).

Two models of a bipedal and a quadrupedal robot are treated here. The presented approach, however, is applicable to any other legged robot design.

Our model for the Sony quadruped (see Fig. 1) consists of a 9-link tree-structured multibody system with a central torso and 4 two-link legs. Each leg contains a 2 DoF (degrees of freedom) actuated universal joint in the hip and a 1 DoF actuated rotational joint in the knee (Fig. 1, right). A minimum set of coordinates consists of 18 position and 18 velocity states $(\mathbf{q}(t), \dot{\mathbf{q}}(t))$ which include three Bryant Euler angles for the system orientation, a three-dimensional global position vector, a linear and angular velocity vector, and additionally three angles and their velocities for each leg. The 12 control variables $\mathbf{u}(t)$ correspond to the applied torques in the legs. The kinematical and kinetical data such as length, center of mass, inertia matrix etc. for each robot link have been provided by Sony to the authors.

The biped model used later in the numerical investigations is a planar model with fewer degrees of freedom. It consists of five links with two degrees of freedom in each leg and three degrees of freedom in the reference base-body (torso) for its global position and orientation. Two versions of kinematical and kinetical data of the same biped structure have been investigated. The human-like data used in Sect. 4.2 is taken from [20]. The data of the biped of Sect. 6 is from the humanoid robot design study [23]. The complete set of coordinates consists of 7 position and 7 velocity states $(\mathbf{q}(t), \dot{\mathbf{q}}(t))$. Later in the investigations, it becomes apparent that the lack of a modeled foot is primarily responsible for the biped's highly inefficient operation at high speeds (cf. Sect. 4.2). The foot has a particular important function as its use to propel the body forward during heel-liftoff and to dampen the effects of impulse forces at collision are fundamental for attaining high speed gaits.

The equations of motion are those for a rigid, multibody system experiencing contact forces

$$\begin{aligned} \ddot{\mathbf{q}} &= \mathcal{M}(\mathbf{q})^{-1}\Big(B\mathbf{u} - \mathcal{C}(\mathbf{q},\dot{\mathbf{q}}) - \mathcal{G}(\mathbf{q}) + J_c(\mathbf{q})^T\mathbf{f}_c\Big) \\ 0 &= \mathbf{g_c}(\mathbf{q}) \end{aligned} \tag{1}$$

where n_d equals the number of degrees of freedom in the system, $\mathcal{M} \in \mathbb{R}^{n_d \times n_d}$ is the square, positive-definite mass-inertia matrix, $\mathcal{C} \in \mathbb{R}^{n_d}$ describes the Coriolis and centrifugal forces as well as Coulomb and viscous friction, $\mathcal{G} \in \mathbb{R}^{n_d}$ are the gravitational forces, and $\mathbf{u}(t) \in \mathbb{R}^m$ the control input functions which are mapped with the constant matrix $B \in \mathbb{R}^{n_d \times m}$ to the actively controlled joints. The ground contact constraints $\mathbf{g_c} \in \mathbb{R}^{n_c}$ represent n_c holonomic constraints on the system from which the constraint Jacobian may be obtained $J_c = \frac{\partial \mathbf{g_c}}{\partial \mathbf{q}} \in \mathbb{R}^{n_c \times n_d}$, while $\mathbf{f}_c \in \mathbb{R}^{n_c}$ is the ground constraint force. Note: If the constraint Jacobian J_c is rank-deficient, then a new matrix J_c' may be constructed from J_c using only the linear independent rows. In general form, the system dynamics (1) results in a system of differential-algebraic equations (DAEs) of (differential) index 3.

The biped and quadruped are modeled as free-flying systems permitting the modeling of running gaits where all legs might be in a flight phase. It was shown in [9] that numerical interpolation or extrapolation of Euler angles, as might occur in most standard integration schemes, can produce inaccurate results since the interdependencies between the axes are ignored. For simulation purposes, it is thus advisable [9, 47] to use unit quaternions and their time derivatives to represent the system's rotational state coordinates. These introduce two additional algebraic constraints to the dynamic model (1). The desired numerically accuracy may be usually obtained with Euler angles in gait optimizations, however, as the time span is relatively short.

2.2 Constraints

An important aspect of formulating a gait optimization problem is establishing the many constraints on the problem. Legged systems are good examples of hybrid dynamical systems [22] as they periodically enter different discrete states which in turn (discontinuously) switch the dynamical model. These occur each time a new contact occurs or a contact is freed. The numerical solution of hybrid optimal control problems (HOCP) is still in its early stages [5, 51], yet when the discrete trajectory (contact events) is previously specified, current numerical solution techniques have been shown to work well [7, 21].

For a biped, specifying the order of contact events is not a problem as one need only distinguish between walking and running. The range of different quadruped gaits, however, can be quite large. The problem of searching over all possible gaits in a gait optimization problem has not yet been completely solved [22]. Biological studies can provide a good indication, though, as to which quadrupedal gaits are the most efficient for different forward velocities [2]. A numerical advantage for considering gaits with the left and right legs of a pair with equal duty factors is that the problem can be completely formulated within half a gait cycle. Both symmetric and asymmetric gaits fit within this framework as we make no restriction on the relative phases of each leg. (In a symmetric gait, one leg of a leg pair makes ground contact half a gait period after the other leg). In nature, it may be witnessed that asymmetric gaits are more prevalent with quadrupeds when moving at faster speeds.

A summary of the modeling constraints for a *complete* gait cycle is as follows.

Periodic gait constraints (enforced during gait optimization):

1. Periodicity of continuous state and control variables,

$$\mathbf{q}(t_f) = \mathbf{q}(0), \quad \dot{\mathbf{q}}(t_f^+) = \dot{\mathbf{q}}(0)\,. \tag{2}$$

2. Periodicity of ground contact forces,

$$\mathbf{f_c}(t_f^+) = \mathbf{f_c}(0)\,. \tag{3}$$

The notation $\dot{\mathbf{q}}(t_f^+)$ and $\mathbf{f_c}(t_f^+)$ indicates the state velocity and contact force vectors immediately after any collision or impluse events occurring at the final time of the gait cycle $t = t_f$. The periodic constraints differ for a half a gait cycle when left and right legs of a pair have equal duty factors in that individual components of the above vectors will be equal to the negative of its initial value.

Exterior environmental constraints:

1. Kinematic constraints on the height (z-coordinate) of the sole of the swing leg's foot.
The sole's height $q_{sole,z}$ is calculated from a forward kinematics function $FK(\cdot)$ of the position states $\mathbf{q}$,

$$q_{sole,z} = FK(\mathbf{q}(t)) \geq 0\,. \tag{4}$$

In the case of unlevel ground, the 0 may be replaced by a ground height function of the horizontal position of the swing leg tips. In these investigations, we consider only level ground.

2. Ground contact forces lie within the friction cone and unilateral contact constraints are not violated [15, 43].
In the case of point contact, ground linear contact forces $\mathbf{F} = [F_x\ F_y\ F_z]^T$ must satisfy (otherwise a slipping contact state is entered),

$$\sqrt{F_x^2 + F_y^2} \leq \mu_t F_z, \qquad F_z \geq 0\,, \tag{5}$$

with friction coefficient μ_t. The contact force vector $\mathbf{f_c}$ which appears in (1) includes the contact linear force vectors $\{\mathbf{F}_j\}$ from each contact leg j.
In the case of multiple contact, such as a foot lying flat on the ground, the rotational contact force pointing in the normal direction to the foot T_z is constrained by the product of a friction coefficient μ_d and F_z,

$$|T_z| \leq \mu_d F_z\ . \tag{6}$$

Interior modeling constraints:

1. Jump conditions in the system velocities due to inelastic collisions of the legs with the ground.
If the exterior constraint (4) is violated, a collision occurs. This is modeled as an instantaneous jump in the state velocities at the k-th such collision or contact event,

$$\dot{\mathbf{q}}(t_{S,k}^+) = Jump_{q,q'}(\mathbf{q}(t_{S,k}^-), \dot{\mathbf{q}}(t_{S,k}^-))\,, \tag{7}$$

where $\mathbf{q}(t_{S,k}^-)$ and $\dot{\mathbf{q}}(t_{S,k}^+)$ indicate the values of $\mathbf{q}$ just before and after the collision event respectively. The function *Jump* calculates the jump in the state velocities resulting from the point of collision instantaneously reaching a zero velocity. The jump is physically modeled as the consequence of an impulsive force propagating throughout the system which may be calculated using the law of conservation of angular momentum [7, 21]. This approach is a numerically tractable approximation to real collision phenomena.

2. Magnitude constraints on states, controls and control rates,

$$L_{\mathbf{q}} \leq \mathbf{q} \leq U_{\mathbf{q}} \qquad L_{\dot{\mathbf{q}}} \leq \dot{\mathbf{q}} \leq U_{\dot{\mathbf{q}}} \qquad L_{\mathbf{u}} \leq \mathbf{u} \leq U_{\mathbf{u}} \qquad L_{\dot{\mathbf{u}}} \leq \dot{\mathbf{u}} \leq U_{\dot{\mathbf{u}}} \ . \tag{8}$$

$L_{(\cdot)}$ and $U_{(\cdot)}$ are constant, real vectors of length equal to their arguments.

3. Actuator torque-speed limitations.
The applied torque at the actuated joint i is constrained by the characteristic line of the motor-gear train,

$$|u_i| \leq (\dot{\theta}_{max,i} - |\dot{\theta}_i|)\frac{G_i^2 \eta_i}{m_i} \ , \tag{9}$$

where u_i is the applied torque at joint i, $\dot{\theta}_i$ and $\dot{\theta}_{max,i}$ are the joint i velocity and maximum absolute joint velocity respectively, G_i is the gear ratio, η_i is the gear efficiency, and m_i is the slope of the motor characteristic line.

Simulation of legged locomotion must not only enforce the interior constraints but must also supervise the environmental constraints. When the latter can no longer be enforced, the system enters a new discrete state often leading to a switch in the dynamical model (e.g. in $\mathbf{g_c}(\mathbf{q})$, $J_c(\mathbf{q})$ of Eq. (1)) and system state, which in turn must reflect the internal modeling constraints.

The topic of multiple unilateral contact constraints in a rigid body as commonly encountered between the three-dimensional model of biped feet and the ground, have recently received increasing attention [43], and elegant numerical solution methods now exist so that such problems may be solved in real-time applications [15]. Solutions to similar problems with a rigid body experiencing multiple collisions have been treated in [48].

2.3 Robotic Dynamic Algorithms

Symbolic multibody algorithms can construct efficient, closed form dynamics of $\mathcal{O}(N)$ complexity for a legged system through symbolic simplifications [36, 41]. Their purpose is to develop efficient dynamic equations for specific multibody systems. This approach is not well-suited to legged systems due to the switching characteristic of the dynamics in different contact states, varying parameter and exterior load conditions. The Composite Rigid Body Algorithm (CRBA) [24, 38, 54] is an approach which numerically solves the equations of motion by efficiently constructing the entire mass-inertia matrix $\mathcal{M}$ with $\mathcal{O}(N^2)$ complexity where N is the number of links in the system. It satisfies the prerequisite for an easy change of parameters or the introduction of external forces without making changes to the algorithm. Further descriptions of these algorithmic approaches may be found in [46] where they are also associated with commercial packages. These solution methods are, in general, superceded in modularity and in efficiency for systems with more than 7–8 links by the articulated body algorithm (ABA) [13].

The $\mathcal{O}(N)$ ABA [12, 44] has been shown to be a very exact and numerically stable multibody algorithm superior to the CRBA as it introduces less cancellations of terms [42]. It exploits the linear relationship between accelerations in a rigid-body system and the applied forces; in particular, the definition of the articulated body inertia, the inertia of the 'floppy' outboard chain of rigid bodies not subject to applied forces, has permitted the construction of a recursive algorithm for the forward dynamics [12]. The similarities to the Kalman filtering and smoothing algorithms led to an alternative decomposition of the mass-inertia matrix, which in turn led to an $\mathcal{O}(N)$ closed-form expression for the inverse mass matrix [44]:

$$\begin{array}{rcll} \mathcal{M} & = & H^T \phi^T M \phi H & \text{(Newton-Euler Factorization)} \\ \mathcal{M} & = & [I + K\phi H]^T D [I + K\phi H] & \text{(Innovations Factorization)} \\ \mathcal{M}^{-1} & = & [I - K\psi H] D^{-1} [I - K\psi H]^T \ . & \end{array} \tag{10}$$

Let n_{d_i} equal the motion degrees of freedom for link i. Then $n_d = \sum_i n_{d_i}$ and the matrix $H = \text{diag}\{H_i\}$ contains the $6 \times n_{d_i}$ matrices H_i which span the motion freedom subspace of joint i. In the case of a 1 DoF joint, it merely describes the joint's axis of motion. The $6N \times 6N$ lower triagonal matrix ϕ contains all the (6×6) operators $\phi_{i,i-1}$ describing the transformations of six-dimensional spatial velocity vectors corresponding to any two links that lie on a path from the base to the branch tips. Its lower triangular form induces the base-to-tip recursion and the

LDL^T structure to the factorization of $\mathcal{M}$. The matrix $M = \text{diag}\{M_i\}$ contains the 6×6 spatial inertia matrices of each link M_i represented at joint i.

The 6×6 articulated body inertias P_i satisfy a Riccati equation identical to that found in the discrete-time Kalman filter with tip-to-base recursion instead of a time iteration,

$$
\begin{array}{l}
\textbf{for i} = \textbf{N}, ..., \textbf{1} \\
\quad \psi_{i+1,i} = \bar{\tau}_{i+1}\phi_{i+1,i} \\
\quad P_i = \psi_{i+1,i}^T P_{i+1}\psi_{i+1,i} + M_i \\
\quad D_i = H_i^T P_i H_i \\
\quad G_i = D_i^{-1} H_i^T P_i \\
\quad \bar{\tau}_i = I - H_i G_i \\
\textbf{end loop}
\end{array}
\tag{11}
$$

From the above operator definitions, new operator identities may be established which result in the alternative innovations factorization [20, 44]. The matrix $D = \text{diag}\{D_i\}$ contains the nonsingular $n_{d_i} \times n_{d_i}$ operators D_i which are the articulated body inertias along each joint's motion degrees of freedom. The recursion operator ψ containing the (6×6)-matrices $\psi_{i,i-1}$ have the same structure as ϕ and $\phi_{i,i-1}$ and are obtained by projecting $\phi_{i,i-1}$ using the 6×6 operator $\bar{\tau}_i$ onto the articulated motion subspace. The $n_{d_i} \times 6$ dimensional matrices $K_i = G_i\phi_{i,i-1}$ may be collected into one $(n_d \times 6N)$-matrix $K = \text{subdiag}\{K_i\}$ so that the complete recursion above may be represented in the succinct form of (10). In [42] it was shown how this algorithm may be obtained using block matrix elimination from a matrix representation of the CRBA.

There also exist various methods for solving the forward dynamics problem subject to contact constraints (1). For systems with few contact constraints n_c relative to the number of bodies N in the system as is the case with legged systems, the best suited approach is to solve first for the contact constraint forces $\mathbf{f}_c$, and then to substitute these to solve for the accelerations $\ddot{\mathbf{q}}$ [13]. It is not only computationally advantageous, but also lends itself well to a recursive algorithmic approach. These algorithms with slight numerical modifications are described in [20], where they were used for optimization purposes. An object-oriented C++ toolbox also based on these algorithms is described in [25].

Other $\mathcal{O}(N)$ algorithms also exist which do not depend on the ABA such as that using natural coordinates [11, 35]. This approach provides a more systematic way of dealing with systems with many closed kinematic loops and additional algorithms exist within this framework for deriving exact sensitivities to the dynamics. The ABA is superior in modularity and efficiency to that of natural coordinates which is of primary importance in legged systems. Additionally, recursive algorithms also exist for calculating exactly the sensitivities to the dynamics in the ABA framework [32] which can be valuable for evaluating gait stability in legged systems as well as for optimization of gait trajectories. The modularity of the ABA also allows for its straightforward extension to include many other modeling complexities such as, for example, geared actuation [30], underactuation [31], and even an $\mathcal{O}(log(N))$ parallel implementation [14].

2.4 Reduced Dynamics

It is possible to calculate the contact dynamics using a reduced dynamics algorithm. This approach, also known as coordinate partitioning [1], projects the dynamics (1) onto a reduced set of independent states thus converting the DAE contact system (1) into an ODE system of minimal size. Using a recursive multibody algorithmic approach, the reduced dynamics may be evaluated without explicitly constructing them [21]. This approach requires solving the inverse kinematics problem for the dependent states which, in the case of legged systems, are generally the contact leg states. For most leg configurations, this problem is easily solved using knowledge of the relative hip and foot contact locations. This approach is not an approximation to the dynamics but rather a more efficient computational method.

The position state vector $\mathbf{q}$ may be partitioned into independent position states $\mathbf{q}_1$ and dependent position states $\mathbf{q}_2$ which may be obtained from $\mathbf{q}$ via a linear transformation, $\mathbf{q}_1 = Z\mathbf{q}$. The transformation $Z \in \mathbb{R}^{(N-n_c)\times N}$ is in the case of legged systems a constant full-rank matrix consisting of unit vectors or $\mathbf{0}$. It is assumed that an explicit function $i(\cdot)$ exists which determines the dependent position states $\mathbf{q}_2$ from $\mathbf{q}_1$, i.e. $\mathbf{q}_2 = i(\mathbf{q}_1)$. In the case of legged systems, an inverse kinematics solution generally exists for the dependent contact leg states given the hip position $\mathbf{p}_h$ and the foot contact position $\mathbf{p}_c$ in inertial coordinates where $\mathbf{p}_h$ is a function of $\mathbf{q}_1$. For succinctness, we write $i(\mathbf{q}_1) = i(\mathbf{p}_h(\mathbf{q}_1), \mathbf{p}_c)$. One may partition the constraint velocity equation $J_c\,\dot{\mathbf{q}} = \mathbf{0}$ with respect to the independent $\dot{\mathbf{q}}_1$ and dependent velocity states $\dot{\mathbf{q}}_2$, $J_{c,1}\dot{\mathbf{q}}_1 + J_{c,2}\dot{\mathbf{q}}_2 = 0$. This similarly provides a change of variables for the velocity states,

$$
\dot{\mathbf{q}}_1 = Z\dot{\mathbf{q}}, \quad \dot{\mathbf{q}}_2 = -J_{c,2}^{-1}J_{c,1}\dot{\mathbf{q}}_1 \ . \tag{12}
$$

Substituting $\mathbf{q}_1$, $\mathbf{q}_2$, $\dot{\mathbf{q}}_1$, and $\dot{\mathbf{q}}_2$ into (1) and multiplying (1) by Z then gives an ODE of size $(N - n_c)$

$$\ddot{\mathbf{q}}_1 = Z\mathcal{M}(\mathbf{q}_1, i(\mathbf{q}_1))^{-1}\Big(B\mathbf{u} - \mathcal{C}(\mathbf{q}_1, i(\mathbf{q}_1), \dot{\mathbf{q}}_1, -J_{c,2}^{-1}J_{c,1}\dot{\mathbf{q}}_1) - \mathcal{G}(\mathbf{q}_1, i(\mathbf{q}_1)) + J_c^T\mathbf{f}_c\Big) \ . \tag{13}$$

The principal advantage of this approach is that one needs only perform the optimization on the reduced dimensional state. The state must then be monitored such that it remains within a well-defined region of the state space. In Sect. 4.2, where the optimal amble gait is investigated for a quadruped, there are always two legs in contact. As a result, instead of the full 36 states $(\mathbf{q}, \dot{\mathbf{q}})$, 24 states can describe the system.

The numerical advantages can be considerable. The general, 'index 3' DAE system (1) for legged robots must otherwise be converted to a 'index 1' system requiring the formulation of additional algebraic equations based on the dynamics. Additionally, special-purpose DAE optimization/simulation tools are required which are not as mature as their ODE counterparts.

3 Dynamic Stability and Performance

3.1 Measures of Stability

Stability plays a critical role in bipedal and quadrupedal locomotion. A nontrivial observation is that there is usually a small margin in the legged system state space between a physically realizable periodic motion and kinematically or dynamically unstable configurations. Kinematic instability refers to when the ground projected system center of mass (GCoM) lies outside the convex hull of the leg support points (known as the 'support polygon'). Dynamic instability occurs when the system is in a configuration for which an actuation strategy does not exist which can prevent the system from falling. The dynamically unstable region of the state space is a subset of the kinematically unstable region. The kinematic and dynamic stable regions may be defined as the complements of their respective unstable regions. The motions developed at the TU Darmstadt [10] and other teams in the RoboCup competition for the Sony four-legged robots (Fig. 1) enforce kinematic stability which is more robust yet slower due to the stringent actuation constraints. The generation of faster movements thus requires the extension to dynamic stability.

Definitions of static stability margins usually concern the minimum distance between the GCoM and the support boundary. The slow, conservative motions characteristic of enforcing static stability have been slightly improved in physical legged systems [26, 40, 28] by enforcing the zero-moment-point (ZMP) [53] to lie within the support polygon. The ZMP is that point on the ground where the total moment generated due to gravity and inertia equals zero or equivalently the point where the net vertical ground reaction force acts. As pointed out in [17], this point cannot leave the support polygon and, in the case when the foot is rotating about the toe or heel, it lies directly on the edge of the support polygon. During these periods, the ZMP does not indicate the amount of instability in the system. The period of foot rotation is approximately 80% of a normal human walking gait demonstrating that to achieve similar motions with legged machines, improved quantitative measures of stability are required. Within the large variety of possible quadrupedal gaits (pace, gallop, amble, ...), there also exist many configurations where the ZMP provides little useful information. An alternative measure proposed in [17] for bipeds (though extendable to quadrupeds) is the foot-rotation-indicator (FRI). This coincides with the ZMP during periods of static equilibrium of the foot and otherwise provides information as to the foot's rotational instability.

In [27], dynamic stability was categorized into postural stability and gait stability. Postural stability is maintained when the posture (torso orientation and position) remains within a bounded range of values. Gait stability refers to the dynamical system definition of stability for limit cycles in periodic gaits. Foot rotation instability measured by the FRI is a more complete measure of postural instability, but it still does not provide any information as to gait stability/instability. Another more recently introduced postural stability measure for quadrupeds uses the angular momentum about the support edges [37] to define a stability index. Like the FRI, this method can provide both directional information and a reference stability quantity that can be used to quantify system instability. Though postural stability measures are not rigorous measures for the stability of a dynamical system, these measures provide a means to monitor the stability or instability present in legged systems. Another advantage is that these measures may be directly incorporated into controllers for *on-line* use and, additionally, they can treat aperiodic gaits, a necessity in an environment containing obstacles.

When considering full-dimensional dynamical models, gait stability measures must be calculated using numerical methods. For higher dimensional systems, numerical methods and nonlinear dynamical systems theory, in particular Floquet theory, can provide a means for evaluating gait stability [29, 39]. The eigenvalues (Floquet multipliers) of the sensitivity matrix (monodromy matrix) between the final state values $\mathbf{x}(t_f)$ and the initial state values $\mathbf{x}(0)$ of the optimization problem (cf. Sect. 4.2) characterize the stability of the periodic system. The eigenvalues are equivalent to the linearized Poincaré map and indicate asymptotic *open-loop* stability when they

are less than unity. An optimization of these eigenvalues with respect to a high dimensional dynamical model is not expected to be successful due to the problem nonconvexity and the high dimensional nonlinear dynamics. We may calculate, however, the maximum Floquet multiplier obtained from an optimization in order to evaluate its open-loop orbital stability with respect to different performance measures. This approach is used in Sect. 4.2.

3.2 Measures of Energy and Efficiency

In autonomous legged systems, the measurement and control of expended or lost energy can be nearly as important as stability. A challenge of systems with limited power supply is to combine energy conserving motion with the robustness and stability properties discussed previously. It has been additionally witnessed in humans that steady-state forward walking approximates a minimum energy motion according to a dynamical model for the human body [45]. In this sense, an attempt to reproduce smooth, natural motion will also take these factors into account. Sect. 3.3 presents two different forms of energy measurements that may be used to measure performance. One measure considers the largest form of energy loss, Joule thermal loss [34], found in many actuated robotic systems. It is a generalization of the common technique of minimizing the integral of squared applied torques. The other technique is to measure directly efficiency as introduced in [18]. Here the normalized output power is measured.

3.3 Performance Specifications

Performance functions are functionals of the control actuation or of dynamic quantities and may be used to measure desirable aspects of legged motion. The performance functions presented here for the study of periodic gaits can measure the stability/instability or energetical efficiency of the periodic motion. These performance measures are not explicitly dependent on the time period of the gait so that they may be used in on-line calculations as well as in numerical optimization approaches for obtaining dynamically stable motions for bipeds and quadrupeds.

Stability Performance 1:

The **FRI** point may be computed as that point for which the net ground tangential impressed forces (FI_x, FI_y) acting on the foot are zero. These forces are the acting forces and may differ from the constraint forces $\mathbf{F} = [F_x \; F_y \; F_z]^T$ [17]. If N_f feet/leg-tips are in contact with the ground, **FRI** may be considered as the net point of action for all ground impressed forces resulting from the robot gravity and inertial forces. It may be computed using the rotational static equilibrium equation for the feet,

$$\sum_{j=1}^{N_f} \left(\mathbf{n}_j + \mathbf{FO}_j \times \mathbf{f}_j - \mathbf{FG}_j \times m_j \mathbf{g} \right)_t = 0 \; , \tag{14}$$

where $\mathbf{n}_j$ and $\mathbf{f}_j$ are the moment and linear force vectors from contact foot j acting on its connecting point $\mathbf{O}_j$ to the remainder of the robot, $\mathbf{FO}_j$ and $\mathbf{FG}_j$ are the vectors from **FRI** to $\mathbf{O}_j$ and the foot center of mass $\mathbf{G}_j$ respectively, m_j is the foot mass, and $\mathbf{g}$ is the gravity vector. The subscript t indicates that only the ground tangential x- and y-coordinates must satisfy the equality.

A stability performance index appropriate for maximizing postural stability is the average distance in the ground plane between the point **FRI** and the ground projected center of mass **GCoM**

$$\mathbf{J}_{s1}[\mathbf{q}, \dot{\mathbf{q}}, \mathbf{u}] = \int_0^{t_f} ((\mathrm{GCoM}_x - \mathrm{FRI}_x)^2 + (\mathrm{GCoM}_y - \mathrm{FRI}_y)^2) \, \mathrm{d}t \quad \longrightarrow \quad \min! \tag{15}$$

Stability Performance 2:

The measure proposed in [37] is an alternative measure based on the angular momentum and it takes into consideration the momentum of the swing legs. It is however limited to quadrupedal gaits with at least two legs in contact with the ground. The stability/instability margin is equal to

$$S_H = \min\{S_H^l, \; l = 1, \ldots, n_l\} \, , \tag{16}$$

where n_l is the number of edges in the support polygon. The stability values S_H^l for each edge depend on whether the edge is a diagonal or non-diagonal edge. The linear and angular momentum of the system about the system center of mass **CoM** are denoted as $\mathbf{L_{CM}}$ and $\mathbf{H_{CM}}$ respectively. These values can be used to compute the angular momentum about a point **P** on the ground using the transformation $\mathbf{H_P} = \mathbf{H}_{CM} + \mathbf{r}_{P,CM} \times \mathbf{L}_{CM}$ where $\mathbf{r}_{P,CM}$ is

the vector from **P** to **CoM**. When **P** lies on the edge connecting two support legs, the rotational tendency about that edge is

$$H_l = (\mathbf{H}_{CM} + \mathbf{r}_{P,CM} \times \mathbf{L}_{CM}) \cdot \hat{\mathbf{e}}_l$$

where $\hat{\mathbf{e}}_l$ is the unit vector along edge l [37]. The reference angular momentum H_l^{ref} about edge l is defined as the minimum angular momentum to tip over the edge if the system were an inverted pendulum,

$$H_l^{ref} = (\mathbf{r}_{l,CM} \times m_{total}\mathbf{v}_{ref}) \cdot \hat{\mathbf{e}}_l \ .$$

Here $\mathbf{r}_{l,CM}$ is the orthogonal vector from the edge l to **CoM** and m_{total} is the total system mass. The reference velocity vector $\mathbf{v}_{ref}$ is computed from the kinetic energy required to attain the higher potential energy at which the system **CoM** would lie above edge l, $m_{total}(g\|\mathbf{r}_{l,CM}\| \cos\psi_l - \mathbf{g}^{\mathbf{T}}\mathbf{x}_{CM})$, where $\mathbf{g} = [\,0\ 0\ g\,]^T$ is the gravitational force vector. Then for a non-diagonal edge, $S_H^l = H_l^{ref} - H_l$.

In the case of a diagonal edge, the maximum angular momentum is defined as

$$H_l^{max} = (\mathbf{r}_{l,CM} \times m_{total}\mathbf{v}_{tip}^{max}) \cdot \hat{\mathbf{e}}_l$$

where $\mathbf{v}_{tip}^{max}$ is the maximum velocity vector of the swing leg's tip. If only two legs are in contact, then when the **CoM** has not yet crossed the diagonal edge then $S_H^l = \min\,(H_l - H_l^{ref}, H_l^{max} - H_l)$, and if it has crossed $S_H^l = H_l^{max} - H_l$. In the case of a third supporting leg behind the diagonal edge $S_H^l = H_l^{max} - H_l$, and if the supporting leg lies in front then $S_H^l = H_l^{ref} - H_l$. An overall gait stability measure may also be constructed from the above when dealing with a periodic gait by defining it to be the minimum value of S_H over the entire gait cycle or its integrated value. As stability is more of a risk criterion than a cost criterion, the minimum value formulation is used here.

The objective is the min-max criterion:

$$\min_{0\le t\le t_f} S_H(t) \longrightarrow \max! \tag{17}$$

Similar to the optimal windshear control problem solved in [4], by adding an additional control parameter p_1 to the problem, the min-max problem may be transformed to a standard form of Mayer-type objective, $p_1 := \min_{0\le t\le t_f} S_H(t)$, where an additional inequality constraint is needed, $S_H(t) - p_1 \ge 0$ $(0 \le t \le t_f)$, and the performance index becomes

$$\mathbf{J}_{s2}[\mathbf{p}] = -p_1 \quad \longrightarrow \ \min! \tag{18}$$

Energy Performance 1:

In the case of robots where a high torque is generated by a large current in the motor, the primary form of energy loss is called the Joule thermal loss [34] and may be calculated as

$$E_J = \int_0^{t_f} \sum_{i=1}^{N} R_i \left(\frac{u_i}{G_i K_i}\right)^2 \mathrm{d}t\,, \tag{19}$$

where R_i, G_i, and K_i are the armature resistance, gear ratio, and torque factor for link i respectively. The energy consumption may then be minimized in the performance by dividing it by the forward distance $S_{FD} > 0$ traveled during one gait cycle,

$$\mathbf{J}_{e1}[\mathbf{u}] = \frac{E_J}{S_{FD}} \quad \longrightarrow \ \min! \tag{20}$$

Energy Performance 2:

Another efficiency cost criterion is the specific resistance ϵ as used in [18]. This measures the output power in relation to the mass moved and the velocity attained and is a dimensionless quantity. By minimizing its integral over the gait cycle, a normalized form of the kinetic energy is minimized,

$$E_\epsilon = \int_0^{t_f} \frac{\sum_{i=1}^{N} |u_i \dot{\theta}_i|}{mgv} \tag{21}$$

where mg is the weight of the system, $\dot{\theta}_i$ is the joint i angle velocity contained within the velocity state vector $\dot{\mathbf{q}}$, and v is the forward velocity. The performance index is then

$$\mathbf{J}_{e2}[\mathbf{q}, \dot{\mathbf{q}}, \mathbf{u}] = E_\epsilon \quad \longrightarrow \ \min! \tag{22}$$

4 Numerical Optimization and Investigations

The optimization of the stability or energy performance indices of Sect. 3.3 subject to the system dynamics and constraints of Sect. 2 leads to optimal control problems. The ODE system (13) for the indepent state variables $\mathbf{q_1}$ can be transformed into first order standard form $\dot{\mathbf{x}}(t) = \mathbf{f}(\mathbf{x}(t), \mathbf{u}(t), t)$ by $\mathbf{x} = (\mathbf{q_1}, \dot{\mathbf{q}}_\mathbf{1})$. Although the computation of the optimal, state feedback control is the ultimate goal where the control is a function of the system state vector $\mathbf{x}$, $\mathbf{u}^*(\mathbf{x})$, it cannot be computed directly because of the system's dimension, nonlinearity and constraints. However, with the help of numerical optimization methods developed during the last decade, optimal open loop trajectories $\mathbf{x}^*(t)$, $\mathbf{u}^*(t)$, $0 \le t \le t_f$, can nowadays be computed efficiently [3].

4.1 Optimization Framework

The optimization we are faced with is to find the unknown open-loop state and control trajectories $(\mathbf{x}(t), \mathbf{u}(t))$ which minimize a performance function $\mathbf{J}$ subject to a set of possibly switching differential equations, nonlinear inequality and equality constraints, and boundary conditions:

$$\dot{\mathbf{x}}(t) = \begin{cases} f^1(\mathbf{x}(t), \mathbf{u}(t), \mathbf{d}(t), \mathbf{p}, t), & t \in [t_0, t_{S,1}], \\ f^k(\mathbf{x}(t), \mathbf{u}(t), \mathbf{d}(t), \mathbf{p}, t), & t \in [t_{S,k-1}, t_{S,k}],\ k = 2, \ldots, m-1 \\ f^m(\mathbf{x}(t), \mathbf{u}(t), \mathbf{d}(t), \mathbf{p}, t), & t \in [t_{S,m-1}, t_f], \end{cases}$$

$$\begin{array}{lcll} g_i^k(\mathbf{x}(t), \mathbf{u}(t), \mathbf{d}(t), \mathbf{p}, t) & \ge & 0, \quad t \in [t_{S,k-1}, t_{S,k}], & i = 1, \ldots, n_{g_m^k},\ k = 1, \ldots, m, \\ h_i^k(\mathbf{x}(t), \mathbf{u}(t), \mathbf{d}(t), \mathbf{p}, t) & = & 0, \quad t \in [t_{S,k-1}, t_{S,k}], & i = 1, \ldots, n_{h_m^k},\ k = 1, \ldots, m. \end{array}$$

$$\begin{array}{lcl} r_i^1(\mathbf{x}(t_0), \mathbf{u}(t_0), \mathbf{d}_0, \mathbf{p}, 0, \mathbf{x}(t_f), \mathbf{u}(t_f), \mathbf{d}_f, t_f) & = & 0 \qquad i = 1, \ldots, n_{r_m^k} \\ r_i^k(\mathbf{x}(t_{S,k}^-), \mathbf{u}(t_{S,k}^-), \mathbf{d}(t_{S,k}^-), \mathbf{p}, t_{S,k}, \mathbf{x}(t_{S,k}^+), \mathbf{u}(t_{S,k}^+), \mathbf{d}(t_{S,k}^+)) & = & 0 \qquad k = 2, \ldots, m-1 \end{array}$$

The optimal control software DIRCOL [50] uses the method of sparse direct collocation [49] to approximate the piecewise continuous states $\mathbf{x}$, controls $\mathbf{u}$, and constant parameters $\mathbf{p}$ of the optimal control problem. The discrete state trajectory $\mathbf{d} : [0, t_f] \to \mathbb{Z}$, $\mathbf{d}(t) = \text{const}$ if $t_{S,k-1} < t < t_{S,k}$, must generally be provided which leads to a multiphase optimal control problem. The continuous state and control variables are approximated by piecewise polynomials along the subintervals $t \in [t_k^j, t_{k+1}^j]$ of a grid $t_{S,j-1} = t_1^j < t_2^j < \cdots < t_{n_{G,j}}^j = t_{S,j}$ in each phase,

$$\begin{array}{lcll} \tilde{\mathbf{u}}_{app}(t) & = & \beta(t; \hat{\mathbf{u}}(t_k^j), \hat{\mathbf{u}}(t_k^{j+1})), & \beta - \text{linear} \\ \tilde{\mathbf{x}}_{app}(t) & = & \alpha(t; \hat{\mathbf{x}}(t_k^j), \hat{\mathbf{x}}(t_k^{j+1}), f_k^j, f_{k+1}^j), & \alpha - \text{cubic} \end{array} \tag{23}$$

where $f_k^j = f^j(\hat{\mathbf{x}}(t_k^j), \hat{\mathbf{u}}(t_k^j), \mathbf{p}, t_k^j)$. The infinite-dimensional optimal control problem is thereby converted to a large-scale, finite-dimensional constrained nonlinear program (NLP) containing the unknown values for $\mathbf{x}, \mathbf{u}, \mathbf{p}, t_{S,i}, t_f$. The problem is then solved using an SQP-based optimization code for sparse systems SNOPT [16]. After having obtained a solution on a coarse grid, a refinement of the discretization grid is applied. The method has demonstrated remarkable robustness and also provides reliable estimates of the adjoint or costate variables of the optimal control problem. The direct collocation approach handles general nonlinear equality and inequality constraints on the states and controls including magnitude bounds, multiple phases with switching dynamics, jumps in the states and controls, and objectives with continuous and discrete costs [49, 50]. The method is thus equipped to handle the complexities of the walking problem: unknown liftoff times, different ground contact combinations for the legs, discontinuous states at collision times of the legs with the ground, switching dynamics, and actuation limits.

This method of generating optimal reference trajectories was used in [21, 22]. Optimality is according to first-order optimality conditions and can only be established locally. However, it may to be applied to systems of much higher state dimension than standard finite-element approaches can handle, as used for example in [6]. This work is the first in which complete three-dimensional dynamical models are used in the optimization process in the case of the quadruped.

4.2 Numerical Investigations

The goal in our numerical investigations is to generate efficient, stable, and rapid periodic motions for our test platforms of the Sony four-legged robot and our humanoid robot currently under construction (Sect. 6). Some of these objective criteria are weighted stronger than others given the platform and specific task to be fulfilled. Performing a numerical optimization requires a set of starting values (rather than an arbitrary set) to begin the

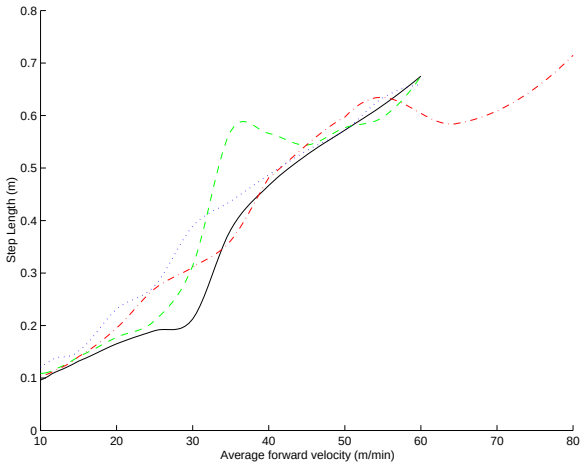

Figure 2: Optimal Step length as a function of average forward velocity for biped robot model. With ankle torques (solid); no ankle torques (dashed); with ankle torques and liftoff force (dashdot); with liftoff force (dotted)

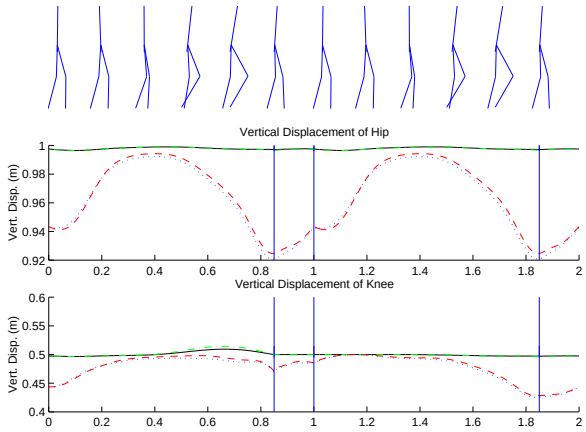

Figure 3: Optimal trajectories of hip and knee vertical positions for biped walking. Walk Speed: 12 *m/min*. No ankle torques (dashed); with ankle torques (solid). Walk Speed: 50 *m/min*. No ankle torques (dotted); with ankle torques (dashdot).

iteration procedure. Due to the complexity of the model, a reasonable set of starting values is required for the iterative optimization procedure to converge to a solution. This can be done in a number of ways. One is to use heuristic arguments to determine a useful guess of the state position paths and feet placement locations, desired forward velocities to determine the state velocities, and desired ground forces with inverse dynamics to calculate a set of control inputs. An alternative is to calculate a series of optimal solutions for related subproblems. The latter approach was the one taken here where first the problem was solved in two dimensions in the saggital plane with most parameters fixed, then all constraints were gradually relaxed using the previous solution to start the subsequent problem. Optimization run times for a single subproblem usually range from 1 to 10 minutes on a Pentium III, 1150 MHz PC.

Based on this numerical and algorithmic framework, a numerical investigation was made into humanoid walking using parameters for the average adult male, for which preliminary results are reported in [21]. Periodic walking trajectories were calculated at a number of different forward velocities by minimizing *Energy Performance 1* including an optimal periodic walk with a forward speed of 12 m/min and a step size of $0.1m$, much smaller than the $0.75m$ witnessed in humans. This study was able to verify that the optimal step length exhibits a roughly linear relationship with increasing average forward velocity (Fig. 2), which has been a standard observation from human walking [45]. We may observe the vertical movement of the hip and knee in Fig. 3. The height of the hip and knees stays roughly at the same level during the slower $12m/min$ optimal walk while during the faster $50m/min$, the well-known sinusoidal motion effect of the hip is more apparent [45]. The system energy has also been shown [21] to reflect the theorized hyperbolic relationship with the forward walking velocity as witnessed in humans [45] according to the formula $E_m = \frac{32}{v} + 0.005\,v$, where E_m is the required energy per meter traveled. Thus, the important observation is made that many human walking characteristics can be generated through an energy minimization of a humanoid multibody dynamic model. Another important conclusion of this investigation is the enormous importance of the rolling action of the foot for rapid and efficient locomotion. Without the foot, these investigations have shown that a double contact phase with both feet on the ground does not provide any locomotive or energetical advantages as an efficient and smooth transfer of the ground contact forces from the existing support leg to the new support leg cannot occur.

In a second set of investigations, dynamically stable quadruped gaits were investigated and both *Energy Performance 1* and *Stability Performance 2* were studied. The solution displayed in Fig. 4 displays two trot gaits advancing at $32\,cm/s$. The one with the lower minimum stability index S_H is purely an energy minimal trot. The other gait optimizes a weighted combination of a stability and energy performance. The energy performance penalizes energy lost per meter traveled so that a forward motion can still be assured. During the fast trot displayed in Fig. 4, it is the small margin between the swing leg's motion and the overall body motion which is responsible for the minimum stability value. At this period of the gait, the body CoG is attempting to cross the diagonal support edge while slowly losing its momentum. The adjacent figure displays the contact configuration during both

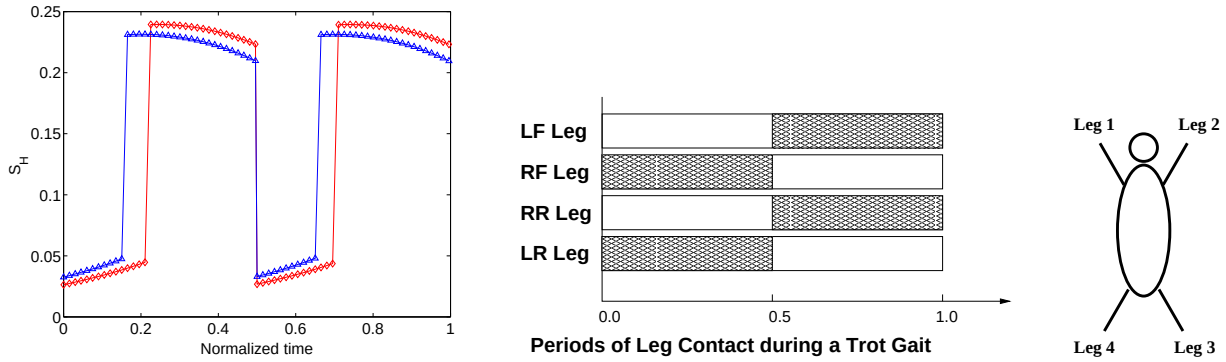

Figure 4: Stability index S_H (left) for an optimized trot gait of a quadruped moving forward at $32\,cm/s$ and $36\,cm/s$ based on a full three-dimensional dynamical model. The sharp increase in the stability index occurs at the instant when the projected CoG passes over the diagonal support edge. The portions of low/high stability indicate a period when the system CoG has not/has passed over the diagonal support edge between the contact legs. The slower gait with the lower minimum stability index is optimized with only an energy performance, while the faster gait is optimized with a weighted max-min stability performance and an energy performance.

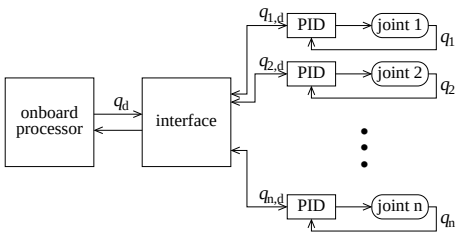

Figure 5: Basic structure of a decentralized trajectory tracking control scheme

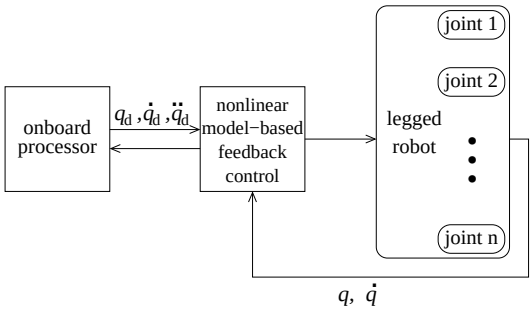

Figure 6: Structure of a centralized, nonlinear model-based feedback control scheme

gaits where the symbols have the following meanings: (LF=left front leg, RF=right front leg, LR=left rear leg, RR=right rear leg).

The purely energy optimal gait travels with an optimal speed of $32\,cm/s$ and a stride length of $9\,cm$. The stability/energy optimal gait travels faster at $36\,cm/s$ with a $10\,cm$ stride length. A typical quadruped trot gait optimization problem according to Sect. 4.1 with 44 grid points contains 1621 NLP variables, 1100 nonlinear equality constraints, and 264 inequality constraints. Run-times averaged 2 minutes on a 1150 MHz PC after having obtained reasonable starting values. A posterior numerical integration of the sensitivity equations (partial derivatives of the state with respect to its initial conditions) for both of the above optimal gaits produced each gait's monodromy matrix. The maximal Floquet multiplier (eigenvalue) of the energy optimal gait was 664, much larger than one, thus far from open-loop asyptotic stability. The combined stability/performance index did, in fact, produce an improvement in the orbital stability measure to 630. This result holds for an angular velocity constraint $|\dot{q}_i(t)| \leq 8\,\mathrm{m/s}$. If $\dot{q}_i$ is not constrained its maximum reaches $24\,\mathrm{m/s}$ and the corresponding maximal Floquet multiplier is about one hundred times larger.

For the application of the quadruped in RoboCup competition (Fig. 1), energy efficiency is not as important since the robot's battery provides sufficient power for the duration of a regulation match. Fast and stable motions are most the important ingredients for success. Compared with the previous four-legged robot dynamic model a main difference is not the overall size but the relatively heavy head which also must be considered.

5 Control of Bipedal and Quadrupedal Robot Motions

Today, most all feedback walking control strategies that have been implemented successfully in three-dimensional humanoid robots or quadrupeds are based on trajectory following control. In trajectory following control, reference trajectories for the body posture, ZMP, or foot flight paths are developed off-line (e.g. through extensive

simulations) and implemented on the bipedal robot using standard controllers such as PID to follow the reference trajectories which have been transformed to desired position (and velocity) information for each of the leg and foot joints (Fig. 5). This strategy has been applied, e.g., to the Honda humanoid robot [26], the Humanoid H6 [40], [28], or [56] for a quadruped. In the case of bipeds, however, forces and moments measured at the foot and angular velocities and linear accelerations measured at the main body usually must be fed back into the control loop to prevent the upper body from losing balance. Feedback linearization techniques (computed torque) are also based on trajectory tracking techniques, yet they take full advantage of a nonlinear dynamical model to arrive at asymptotically stable closed-loop controllers. In contrast to simpler trajectory tracking schemes, these controllers are not decentralized nor decoupled. An example of this type of implementation may be found with Johnnie at the TU Munich [15].

Nonlinear, model-based feedback control methods provide more potential in producing fast, stable motions (Fig. 6). Controllers based on dynamical system properties can provide the means for achieving dynamic stability. However, a highly robust and efficient robot dynamics model enabling real-time computations is needed. The methods described in this paper may serve for this purpose. There are also many control techniques for stabilizing with feedback to previously calculated maximally stable open-loop trajectories, yet this topic extends beyond the scope of this paper.

6 Robot Design and Dynamics of Legged Locomotion

To achieve optimal stability or energetical performance of an autonomous legged robot, especially a humanoid robot, the study of the full dynamics including kinematical and kinetical data must be considered in our opinion already in the design phase of the robot. The selection of motors and gears for the various hip, knee or foot joints of a humanoid must be based on the expected applied force at each joint if the robot is walking or running while further considering the onboard energy supply and other hardware. These forces depend not only on the geometry of the robot links and joints but also on the distribution of masses in each part of the robot's body. The faster the robot walks or runs, the stronger the motors and gears that are required. However, stronger motors and gears are also heavier and require more electrical power and, thus, more and heavier batteries. The heavier weight, though, will counteract the ability of fast walking. Thus, the design of a fast walking humanoid must find a good compromise between many different, counteracting objectives!

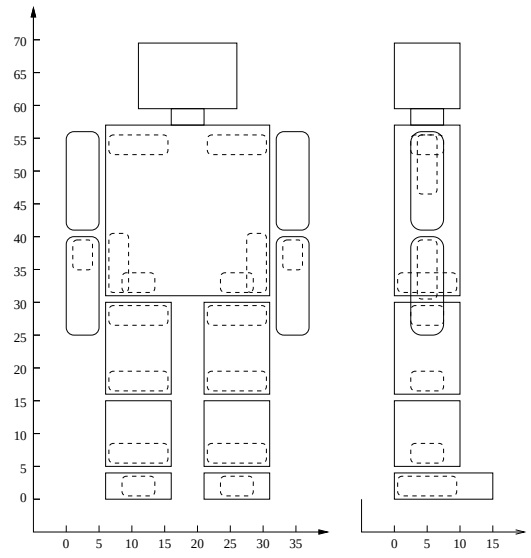

Figure 7: Humanoid Robot Design

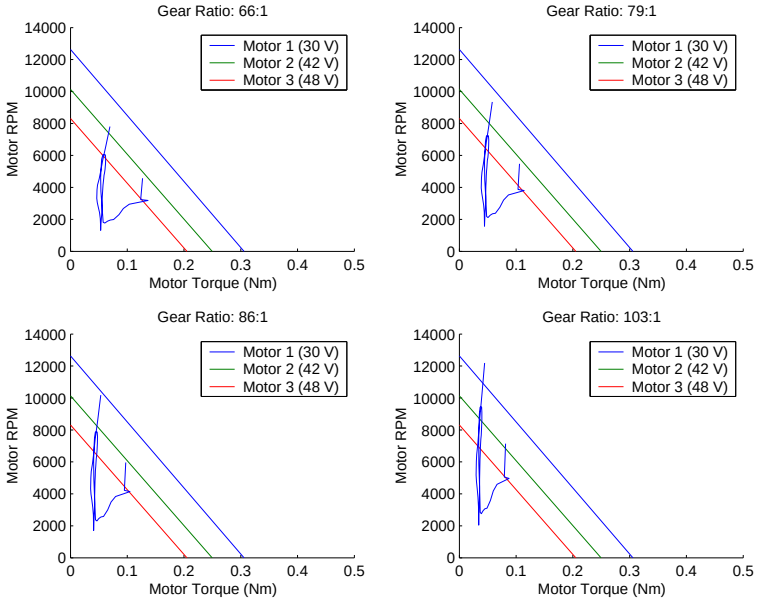

Figure 8: Motor torque vs. rpm from an 18 kg biped

In a design study (Fig. 7), the *Energy Performance 1* is minimized assuming identical and commercially available actuators at all joints for cost and maintenance concerns. An additional constraint is also imposed on the maximum power consumption M_W for each motor. Let $\dot{q}_i$ be the joint i angle velocity, n the total number of

links. Then the optimal control problem is:

$$\min_{\mathbf{u}} \left\{ \int_0^{t_f} \mathbf{u}(t)^T \mathbf{u}(t)\, \mathrm{d}t \right\} \quad \text{subject to} \quad (1) \text{ (or } (13)) \quad \text{and} \quad \max_{t\in[0,t_f],i\in\{1,\ldots,n\}} |\dot{q}_i(t)u_i(t)| \leq M_W\,. \qquad (24)$$

The required motor torques T_m are calculated from the chosen gear ratio N_i and efficiency h_i, $T_m = \frac{u_i}{N_i\ h_i}$ while the required motor speed n_r is obtained from the gear output speed n_o and gear ratio, $n_r = n_o N_i$. Additionally plotted for each given gear ratio are three different motor voltage ratings: $V_m = \{30\mathrm{V}, 42\mathrm{V}, 48\mathrm{V}\}$ assuming a battery supply voltage of $V_s = 38\mathrm{V}$ delivered by three batteries providing 14.4 V each. The motor characteristic lines in Fig. 8 are calculated by first determining the no-load motor speed n_{mV} from its rated value n_m and adjusted according to the supply voltage V_s, $n_{mV} = n_m \frac{V_s}{V_m}$. The given slope of each motor characteristic line determines the reachable torque and velocity combinations as the set of all points below the line. The desired workspace of the motor thus should lie beneath this line.

The construction of a 70 *cm* humanoid robot prototype has been performed (Fig. 7) based on these numerical results for possible walking speeds of up to 1.5 *km/h* [55]. This investigation led to the choice of 42 *V* motors with 66:1 gear ratios. This numerical work has also served to identify the critical problem in generating dynamically stable legged locomotion in autonomous bipeds. Already at speeds above 1.5 *km/h*, no numerical solutions were obtainable using 20W motors indicating the small control margin existing using current actuation and power supply technology in autonomous legged systems.

7 Conclusion and Extensions

In this paper, the role of nonlinear dynamics in the development, implementation and control of bipedal and quadrupedal robots is investigated. A discussion is provided explaining the choice of robotic dynamics algorithms best suited to legged systems, together with reduced dynamics algorithms which aid in reducing the dimension of optimal control problems formulated in this context.

A powerful and efficient numerical optimization framework is also presented which has been thoroughly tested in previous work in optimal gait planning. Several performance criteria have been presented which serve to either optimize energy or stability in legged systems. A maximum stability criterion can be of primary importance when moving rapidly or when obstacles must be avoided. At other times energy concerns are more important such as in autonomous robot design. The efficient recursive multibody algorithms combined with powerful numerical optimal control software solve energy-based performance criteria whose solutions demonstrate their similarity to human motion and aid in the humanoid construction design. A minimax performance stability criteria is also used for generating maximally stable quadruped gaits. The results must be then combined with trajectory tracking controllers which may additionally incorporate the stability index.

References

1 Ascher, U.M.; Petzold, L.R.: Computer Methods for Ordinary Differential Equations and Differential-Algebraic Equations. SIAM (1998)

2 Alexander, R.: The Gaits of Bipedal and Quadrupedal Animals. International Journal of Robotics Research **3**(2) (1984) 49–59

3 Betts, J.T.: Survey of numerical methods for trajectory optimization. AIAA J. Guidance, Control, and Dynamics **21**(2) (1998) 193–207

4 Bulirsch, R., Montrone, F., Pesch, H.J.: Abort landing in the presence of windshear as a minimax optimal control problem. Part 1: Necessary conditions. Part 2: Multiple shooting and homotopy. J. Optimization Theory and Applications **70** (1991) 1–23, 223–254

5 Buss, M.; Glocker, M.; Hardt, M.; von Stryk, O.; Bulirsch, R.; Schmidt, G.: Nonlinear hybrid dynamical systems: modeling, optimal control, and applications. In: S. Engell, G. Frehse, E. Schnieder (eds.): Modelling, Analysis and Design of Hybrid Systems. Lecture Notes in Control and Information Sciences (LNCIS) **279** (Berlin, Heidelberg: Springer-Verlag, 2002) 311-335

6 Channon, P.H.; Pham, D.T.; Hopkins, S.H.: Variational Approach to the Optimization of Gait for a Bipedal Robot. Journal of Mechanical Engineering Science **210** (1996) 177–186

7 Chevallereau, C.; Aoustin, Y.: Optimal reference trajectories for walking and running of a biped robot. Robotica **19**(5) (2001) 557–569

8 Chow, C.K.; Jacobson, D.H.: Studies of human locomotion via optimal programming. Mathematical Biosciences **10** (1971) 239–306

9 Dam, E.B.; Koch, M.; Lillholm, M.: Quaternions, Interpolation, and Animation. Technical Report DIKU-TR-98/5, Dept. of Computer Science, University of Copenhagen, Denmark (1998) July 17. World Wide Web: `http://www.diku.dk/students/myth/quat.html`

10 Darmstadt Dribbling Dackels. Technische Universität Darmstadt (2002) `http://robocup.informatik.tu-darmstadt.de`

11 García de Jalón, J.; Bayo, E.: Kinematic and Dynamic Simulation of Multibody Systems: The Real-Time Challenge. Springer (1993)

12 Featherstone, R.: *Robot Dynamics Algorithms*, Kluwer Academic Publishers (1987)

13 Featherstone, R.; Orin, D.: Robot Dynamics: Equations and Algorithms. IEEE International Conference on Robotics and Automation (2000) 826–34

14 Featherstone, R: A Divide-and-Conquer Articulated-Body Algorithm for Parallel $\mathcal{O}(log(n))$ Calculation of Rigid-Body Dynamics. Part 1: Basic Algorithm. Part 2: Trees, Loops, and Accuracy. International Journal of Robotics Research **18**(9) (1999) 867–892

15 Gienger, M.; Löffler, K.; Pfeiffer, F.: Towards the Design of a Biped Jogging Robot. IEEE International Conference on Robotics and Automation (2001) 4140–45

16 Gill, P.E.; Murray, W.; Saunders, M.A.: User's Guide for SNOPT 5.3: a Fortran Package for Large-Scale Nonlinear Programming, Mathematics Department, Univ. of California, San Diego (1997)

17 Goswami, A.: Postural Stability of Biped Robots and the Foot-Rotation Indicator (FRI) Point. International Journal of Robotics Research **18**(6) (1999) 523–533

18 Gregorio, P.; Ahmadi, M.; Buehler, M.: Design, Control, and Energetics of an Electrically Actuated Legged Robot. IEEE Transactions on Systems, Man and Cybernetics, Part B **27**(4) (1997) 626–634

19 Grizzle, J.W.; Abba, G.; Plestan, F.: Asymptotically stable walking for biped robots: Analysis via systems with impulse effects. IEEE Transactions on Automatic Control **46** (2001) 51–64

20 M. Hardt, Multibody Dynamical Algorithms, Numerical Optimal Control, with Detailed Studies in the Control of Jet Engine Compressors and Biped Walking. Ph.D. Thesis, Electrical Engineering, University of California San Diego, U.S.A. (1999)

21 Hardt, M.; Helton, J.W.; Kreutz-Delgado, K.: Optimal Biped Walking with a Complete Dynamical Model. IEEE Conference on Decision and Control (1999) 2999–3004

22 Hardt, M.; von Stryk, O.: Towards Optimal Hybrid Control Solutions for Gait Patterns of a Quadruped. In: Armada, M.; González de Santos, P. (eds.): CLAWAR 2000: Int. Conf. on Climbing and Walking Robots (Bury St. Edmunds and London, UK: Professional Engineering Publishing, 2000) 385-392

23 Hardt, M.; Wollherr, D.; Buss, M.; von Stryk, O.: Design of an autonomous fast-walking humanoid robot. In: P. Bidaud, F.B. Amar (eds.): CLAWAR 2002: Int. Conf. on Climbing and Walking Robots (Bury St. Edmunds and London, UK: Professional Engineering Publishing, 2002) 391-398.

24 Haug, E.: Computer Aided Kinematics and Dynamics of Mechanical Systems: Basic Methods. Boston: Allyn and Bacon (1989)

25 Helm, A.; Hardt, M.; Höpler, R.; von Stryk, O.: Development of a Toolbox for Model-Based Real-Time Simulation and Analysis of Legged Robots. To appear in GAMM Conference, Augsburg (2002)

26 Hirai, K.; Hirose, M.; Haikawa, Y.; Takenaka, T.: The Development of Honda Humanoid Robot. IEEE International Conference on Robotics and Automation (1998) 1321–26

27 Hu, J.; Pratt, G.: Nonlinear Switching Control of Bipedal Walking Robots with Provable Stability. Humanoid conference, Boston, U.S.A. (2000)

28 Huang, Q.; Yokoi, K.; Kajita, S.; Kaneko, K.; Arai, H.; Koyachi, N.; Tanie, K.: Planning Walking Patterns for a Biped Robot. IEEE Transactions on Robotics and Automation **116** (1994) 30–36

29 Hurmuzlu, Y.; Basdogan, C.: On the Measurement of Dynamic Stability of Human Locomotion. ASME Journal Biomechanical Engineering **116** (1994) 30–36

30 Jain, A.; Rodriguez, G.: Recursive Dynamics for Geared Robot Manipulators. IEEE International Conference on Decision and Control (1990) 1983–88

31 Jain, A.; Rodriguez, G.: An Analysis of the Kinematics and Dynamics of Underactuated Manipulators. IEEE Transactions on Robotics and Automation **9**(4) (1993) 411–422

32 Jain, A.; Rodriguez, G. Sensitivity analysis of multibody dynamics using spatial operators. Proceedings of the Sixth International Conference on Methods and Models in Automation and Robotics (2000) Miedzyzdroje, Poland, 28-31 Aug., 573–8

33 Kajita, S.; Tanie, K.: Experimental study of biped dynamic walking. IEEE Control Systems Magazine **16**(1) (1996) 13–19

34 Kimura, H.; Shimoyama, I.; Miura, H.: Dynamics in the Dynamic Walk of a Quadruped Robot. Advanced Robotics **4**(3) (1990) 283–301

35 Kraus, C.; Winckler, M.; Bock, H.G.: Modeling Mechanical DAE using Natural Coordinates. Mathematical and Computer Modeling of Dynamical Systems **7**(2) (2001) 145–158

36 Kwatny, H.G.; Blankenship, G.L.: Symbolic construction of models for multibody dynamics. IEEE Transactions on Robotics and Automation **RA-11**(2) (1995) 271–281

37 Koo, T.W.; Yoon, Y.S.: Dynamic instant gait stability measure for quadruped walking robot. Robotica **17** (1999) 59–71

38 McMillan, S.; Orin, D.E.: Forward Dynamics of Multilegged Vehicles Using the Composite Rigid Body Method. IEEE International Conference on Robotics and Automation (1998) 464–470

39 Mombaur, K.D.; Bock, H.G.; Schlöder, J.P.; Longman, R.W.: Human-like actuated walking that is asymptotically stable without feedback. IEEE International Conference on Robotics and Automation (2001) 4128–33
40 Nishiwaki, K.; Sugihara, T.; Kagami, S.; Inaba, M.; Inoue, H.: Online Mixture and Connection of Basic Motions for Humanoid Walking Control by Footprint Specification. IEEE International Conference on Robotics and Automation (2001) 4110–15
41 Otter, M.; Elmqvist, H.; Cellier, F.E.: Modeling of Multibody Systems with the Object-Oriented Modeling Language Dymola. Nonlinear Dynamics **9** (1996) 91–112
42 Pai, D.K.; Ascher, U.M.; Kry, P.G.: Forward Dynamics Algorithms for Multibody Chains and Contact. IEEE International Conference on Robotics and Automation (2000) 857–63
43 Pfeiffer, F.; Glocker, C.: Multibody Dynamics with Unilateral Contacts. Wiley Series Nonlinear Science, New York (1996)
44 Rodriguez, G.; Kreutz-Delgado, K.; Jain, A.: A Spatial Operator Algebra for Manipulator Modeling and Control. International Journal of Robotics Research **40** (1991) 21–50
45 Rose, J.; Gamble, J.G.: *Human Walking*, Baltimore, Williams & Wilkins (1994)
46 Schiehlen, W. (ed.): Advanced Multibody System Dynamics: Simulation and Software Tools. Dordrecht: Kluwer Academic Publ., (1993)
47 Sonnenschein, R.: An Improved Algorithm for Molecular Dynamics Simulation of Rigid Molecules. Journal of Computational Physics **59**(2) (1985) 347–50
48 Stewart, D.E.: Rigid-body dynamics with friction and impact. SIAM Review **42**(1) (2000) 3–39
49 von Stryk, O.: Numerical Hybrid Optimal Control and Related Topics. Habilitationsschrift, Technische Universität München (2000) submitted
50 von Stryk, O.: User's Guide for DIRCOL Version 2.1: A direct collocation method for the numerical solution of optimal control problems. Report, Fachgebiet Simulation und Systemoptimierung, Informatik, Technische Universität Darmstadt (2001) World Wide Web: `http://www.sim.informatik.tu-darmstadt.de/sw/dircol`
51 von Stryk, O.; Glocker, M.: Numerical mixed-integer optimal control and motorized travelling salesmen problems. APII-JESA – European Journal of Control **35**(4) (2001) 519–533
52 Yamamoto, Y.; Fujita, M.; de Lasa, M.; Talebi, S.; Jewell, D.; Playter, R.; Raibert, M.: Development of dynamic locomotion for the entertainment robot – teaching a new dog old tricks. CLAWAR: International Conference on Climbing and Walking Robots (2001) 695–702
53 Vukobratović, M.; Borovac, B.; Surla, D.; Stokić, D.: Biped Locomotion. Dynamics, Stability, Control, and Application. Springer-Verlag, Berlin (1990)
54 Walker, M.W.; Orin, D.E.: Efficient Dynamic Computer Simulation of Robotic Mechanisms. Transactions ASME Journal of Dynamic Systems, Measurement, & Control **104** (1982) 205–211
55 Wollherr, D.; Hardt, M.; Buss, M.; von Stryk, O.: Actuator selection and hardware realization of a small and fast-moving autonomous humanoid robot. In: Proc. 2002 IEEE/RSJ Int. Conf. on Intelligent Robots and Systems (IROS), Lausanne, Switzerland, Sept. 30 - Oct. 4 (2002) 2491-2496
56 Yoneda, K.; Iiyama, H.; Hirose, S.: Intermittent trot gait of a quadruped walking machine dynamic stability control of an omnidirectional walk. IEEE International Conference on Robotics and Automation (1996) 3002–7

Received X 2002, revised Y 2003, accepted Z 2003

Address: Dr. Michael Hardt; Prof. Dr. Oskar von Stryk, Simulation and Systems Optimization Group, Technische Universität Darmstadt, Alexanderstr. 10, D-64283 Darmstadt, Germany, email: {hardt,stryk}@sim.tu-darmstadt.de